

Pathology and Pathophysiology of Inhalational Anthrax in a Guinea Pig Model

Vladimir Savransky,^a Daniel C. Sanford,^b Emily Syar,^b Jamie L. Austin,^b Kevin P. Tordoff,^b Michael S. Anderson,^b Gregory V. Stark,^b Roy E. Barnewall,^b Crystal M. Briscoe,^b Laurence Lemiale-Biérinx,^a Sukjoon Park,^a Boris Ionin,^a Mario H. Skiadopoulos^a

Emergent BioSolutions Inc., Gaithersburg, Maryland, USA^a; Battelle Memorial Institute, Columbus, Ohio, USA^b

Nonhuman primates (NHPs) and rabbits are the animal models most commonly used to evaluate the efficacy of medical countermeasures against anthrax in support of licensure under the FDA's "Animal Rule." However, a need for an alternative animal model may arise in certain cases. The development of such an alternative model requires a thorough understanding of the course and manifestation of experimental anthrax disease induced under controlled conditions in the proposed animal species. The guinea pig, which has been used extensively for anthrax pathogenesis studies and anthrax vaccine potency testing, is a good candidate for such an alternative model. This study was aimed at determining the median lethal dose (LD₅₀) of the *Bacillus anthracis* Ames strain in guinea pigs and investigating the natural history, pathophysiology, and pathology of inhalational anthrax in this animal model following nose-only aerosol exposure. The inhaled LD₅₀ of aerosolized Ames strain spores in guinea pigs was determined to be 5.0×10^4 spores. Aerosol challenge of guinea pigs resulted in inhalational anthrax with death occurring between 46 and 71 h postchallenge. The first clinical signs appeared as early as 36 h postchallenge. Cardiovascular function declined starting at 20 h postexposure. Hematogenous dissemination of bacteria was observed microscopically in multiple organs and tissues as early as 24 h postchallenge. Other histopathologic findings typical of disseminated anthrax included suppurative (heterophilic) inflammation, edema, fibrin, necrosis, and/or hemorrhage in the spleen, lungs, and regional lymph nodes and lymphocyte depletion and/or lymphocytolysis in the spleen and lymph nodes. This study demonstrated that the course of inhalational anthrax disease and the resulting pathology in guinea pigs are similar to those seen in rabbits and NHPs, as well as in humans.

Bacillus anthracis, the etiologic agent of anthrax, is a spore-forming bacterium that can cause disease in humans via the gastrointestinal, cutaneous, or inhalation route, inhalation being the most lethal. Following inhalation exposure to *B. anthracis*, the disease course in humans is typically biphasic and consists of non-specific initial clinical signs and symptoms, followed by a sudden onset of respiratory distress with dyspnea, stridor, cyanosis, and chest pain (1–5). The onset of respiratory distress is followed by shock and a high likelihood of death, even with treatment. Anthrax is considered a serious biological terrorist threat because of the stability of *B. anthracis* spores, highly lethal effects by the inhalation route, and the relative ease of dissemination.

It is neither feasible nor ethical to perform human trials to support the development of medical countermeasures against anthrax. Therefore, the use of adequate animal models of inhalational anthrax that closely mimic human disease and accurately reflect mechanisms of host-pathogen interaction is critical for the development and licensure of prophylactic or therapeutic countermeasures against the disease. Rabbits and nonhuman primates (NHPs) are generally considered to be the preferred animal models for studies of inhalational anthrax and have been widely used to study disease pathogenesis, examine bacterial characteristics such as virulence, and assess the efficacy of vaccines and therapeutics (6, 7).

Rabbits (8, 9) and NHPs, including rhesus macaques, cynomolgus macaques, and African green monkeys (10–16), are generally accepted as the preferred animal models of inhalational anthrax. They are considered to be predictive of anthrax disease in humans because of their high susceptibility to infection with toxin-producing strains of *B. anthracis*, particularly via the inhalation route. In contrast, mice appear to be equally susceptible to both

toxigenic and nontoxigenic encapsulated strains, suggesting that the polyglutamate capsule of *B. anthracis* is the primary virulence factor in this model and the mechanism of disease is not toxin mediated (17).

The course of inhalational anthrax and pathological changes observed in rabbits and NHPs are similar to those reported in humans. Findings in rabbits include necrotizing lymphadenitis, splenitis, pneumonia, and vasculitis, as well as hemorrhage, congestion, and edema in multiple tissues (8). Similar lesions are observed in NHPs, which also frequently exhibit meningitis (18), thus exhibiting the full range of lesions described in human inhalational anthrax (3).

In certain cases, however, these well-established models do not respond to a specific countermeasure (e.g., a vaccine containing a novel adjuvant) in a manner consistent with the human response and therefore cannot be used to assess the efficacy of such a countermeasure. For example, rabbits do not respond strongly to vaccine adjuvants that act via Toll-like receptor 9 (19). Such cases necessitate the development of an alternative animal model that is

Received 16 November 2012 Returned for modification 2 January 2012

Accepted 12 January 2013

Published ahead of print 28 January 2013

Editor: L. Pirofski

Address correspondence to Mario H. Skiadopoulos, skiadopoulosm@ebsi.com.

V.S. and D.C.S. contributed equally to this study.

Copyright © 2013, American Society for Microbiology. All Rights Reserved.

doi:10.1128/IAI.01289-12

The authors have paid a fee to allow immediate free access to this article.

TABLE 1 Natural history animal group designation and study endpoints

Group	No. of animals/group ^c	Terminal endpoint (time after aerosol exposure)	Telemetry	CBC ^d	Bacteremia	qPCR	PA ELISA	Clinical chemistry/CRP
1	4 (2, 2)	24 ± 1 h		X ^e	X	X	X	X
2	4 (2, 2)	30 ± 1 h		X	X	X	X	X
3	4 (2, 2)	36 ± 1 h		X	X	X	X	X
4 ^a	4 (2, 2)	48 ± 1 h		X	X	X	X	X
5 ^a	4 (2, 2)	60 ± 1 h		X	X	X	X	X
6 ^a	4 (2, 2)	72 ± 1 h		X	X	X	X	X
7 ^a	4 (2, 2)	96 ± 1 h		X	X	X	X	X
8 ^b	9 (4, 5)	14 days	X					
9	4 (2, 2)	0 days (control)		X	X	X	X	X

^a Animals in these groups died prior to the scheduled terminal endpoint.

^b Animals in group 8 implanted with telemetry units were not bled.

^c The values in parentheses are the numbers of males and females, respectively.

^d CBC, complete blood count.

^e X indicates that data were obtained.

predictive of the human response to a particular drug or vaccine yet closely follows the standardized conditions of anthrax exposure that have been established for the rabbit and NHP models (e.g., nose-, muzzle-, or head-only exposure; use of a *B. anthracis* strain virulent in humans; a defined challenge dose of the pathogen, etc.). Investigation of the natural history of the disease under these standardized conditions is an essential part of such model development.

The guinea pig model has been used extensively to elucidate the pathogenesis of inhalational anthrax (20). Exposure of guinea pigs to *B. anthracis* by inhalation or via intratracheal instillation has been shown to result in phagocytosis of spores by alveolar macrophages, followed by intracellular germination and translocation into the thoracic and mediastinal lymph nodes, with subsequent entry of vegetative bacterial cells into the circulation, resulting in massive septicemia and toxemia (20). Thus, the infection mechanism in guinea pigs is very similar to that which is observed in rabbits (8, 21–23), NHPs (15, 24–26), and humans (4, 27, 28). Of note, guinea pigs have been used for anthrax vaccine production and potency assessment (e.g., Sterne vaccine, BioThrax [Anthrax Vaccine Adsorbed]) as part of batch release testing (29), as well as in proof-of-concept studies evaluating the pre- and postexposure efficacy of anthrax countermeasures (23, 30, 31).

Despite the extensive use of guinea pigs in anthrax research, there are no published lethal-dose estimates based on a nose-only aerosol exposure system. The commonly used whole-body aerosol exposure system is not ideally suited for the modeling of a disease where the respiratory system is the primary portal of entry of the causative agent (32). Nose-only exposure limits the entry of the challenge materials to the respiratory tract, avoiding skin contamination, and minimizes oral exposure (33). There are limited data available on the aerosol exposure of guinea pigs to the Ames strain of *B. anthracis*, which has been used in the rabbit and NHP aerosol challenge models (8, 13, 15, 34, 35). Additionally, the Ames strain is highly virulent in humans (36) and is most likely to be the basis of any weaponized strain (37, 38).

This paper describes the determination of the inhaled median lethal dose (LD₅₀) of *B. anthracis* (Ames) spores in guinea pigs using a nose-only aerosol exposure system and the natural history of inhalational anthrax in guinea pigs and discusses the comparability of the guinea pig model to other established animal models and its fidelity to the pathophysiology of the disease in humans.

MATERIALS AND METHODS

Animals. Animal studies were conducted in compliance with the Animal Welfare Act and followed the principles of the Guide for the Care and Use of Laboratory Animals of the National Research Council. The animal procedures were approved by Battelle's Institutional Animal Care and Use Committee. All work was performed in a biosafety level 3/animal biosafety level 3 laboratory registered with the Centers for Disease Control and Prevention and inspected by the Department of Defense and the Department of Agriculture.

Hartley strain guinea pigs weighing between 635 and 874 g (equal numbers of male and female animals) were purchased from Charles River Laboratories (Wilmington, MA). All animals were in good health, free of malformations, and free of clinical signs of disease prior to placement in this study. Animals were individually housed in suspended polycarbonate bedding cages on a stainless steel rack equipped with an automatic watering system. The light-dark cycle was 12 h of each per day, regulated with fluorescent lighting. Manufacturer-tested and certified Guinea Pig Chow pellets (PMI Nutrition International, St. Louis, MO) and water were available *ad libitum*.

Aerosol exposure. *B. anthracis* Ames strain spores were prepared and characterized as described previously (39). Spores were stored at 4 to 8°C in sterile water (Thermo Scientific HyClone, Logan, UT) with 1.0% phenol (Sigma-Aldrich, St. Louis, MO). Prior to use, the spores were washed four times with endotoxin-free water and diluted to the appropriate concentration in endotoxin-free sterile water and 0.01% Tween 20. The spore suspensions contained less than 5% vegetative cells and debris, as confirmed by phase-contrast microscopy (Leica Microsystems, Wetzlar, Germany). Prior to aerosolization, the spores were enumerated and diluted to the proper concentration required to yield the targeted dose.

Aqueous suspensions of *B. anthracis* spores were aerosolized by a six-jet Collison nebulizer and delivered to the guinea pigs using the nose-only aerosol exposure system (CH Technologies Tower, Westwood, NJ). Airflow was regulated using mass flow meters and mass flow controllers to monitor the aerosol flow. The aerosol was sampled for *B. anthracis* viable concentration dose determination using an impinger (model 7541; Ace Glass, Inc., Vineland, NJ). The liquid in the nebulizer and impinger was diluted and enumerated by the spread plate technique to quantify the number of viable bacteria (colony-forming units [CFU]) per milliliter. The inhaled dose was determined on the basis of the calculated bacterial concentration and the animal respiration parameters estimated on the basis of animal weights by using Guyton's formula (40). Prior to exposure, guinea pigs were acclimated to the challenge restraint tubes to reduce animal distress and its potential effect on respiratory parameters. Animals were not anesthetized or sedated during the acclimation or challenge procedure.

TABLE 2 Aerosol challenge and mortality results

Iteration and dosage group	No. of animals	Estimated inhaled dosage (no. of spores/animal)	No. of surviving animals
I			
1	8	3.6×10^4	5
2	8	5.3×10^4	5
3	8	4.8×10^4	5
4	8	4.1×10^4	3
5	8	6.1×10^4	4
6	8	1.1×10^5	2
7	8	3.1×10^5	0
8	8	7.7×10^5	0
II			
9	8	6.6×10^3	8
10	8	7.6×10^3	6
11	8	1.5×10^4	5
12	8	2.3×10^4	4
13	8	4.4×10^4	4
III			
14	8	6.4×10^3	6
15	8	1.0×10^4	8
16	8	2.0×10^4	6
17	8	4.4×10^4	5
18	8	1.0×10^5	5
19	8	2.6×10^5	1
20	8	5.7×10^5	1

LD₅₀ determination. The LD₅₀ was determined by an iterative approach. Three iterations were performed with a total of 160 animals (equal numbers of males and females). Groups of animals were exposed to targeted inhaled doses ranging between 1×10^3 and 1×10^6 spores/animal, with challenge dose levels in the second and third iterations based on the survival results from the previous iteration(s). In each iteration, guinea pigs were monitored for death twice daily for up to 21 days.

The LD₅₀ of inhaled aerosolized anthrax spores was estimated using a probit regression model of the probability of survival at each (log) dose level. All probit models were fitted in SAS (ver. 9.1) using PROC PROBIT (SAS Institute, Cary NC). Model diagnostics were examined to confirm the appropriateness of the model assumptions. Estimated parameters of the probit model were used to compute the LD₅₀ and LD₉₀, and Fieller's method (41, 42) was used to compute a 95% confidence interval for each estimate.

Natural history study. (i) Animals and treatments. Forty-one guinea pigs (20 males and 21 females) were randomly assigned to nine treatment groups as outlined in Table 1. Of these, 37 animals (18 males and 19 females) were exposed via the aerosol route to a target dose of 200 LD₅₀ of *B. anthracis* spores. Nine of the challenged animals (four males and five females) received a surgically implanted telemetry transmitter (TL10M2-C50-PT, Data Sciences International, St. Paul, MN) and were monitored for clinical signs of disease. One group of four animals (two males and two females) was not subjected to aerosol inhalation; these animals were euthanized on day 0 and served as unchallenged controls.

One group of four guinea pigs (two males and two females per group) was scheduled to be euthanized at each of the following postchallenge time points: 24, 30, 36, 48, 60, 72, and 96 h (Table 1). At the specified time point, all surviving animals in the group were exsanguinated and humanely euthanized.

Prior to blood and cerebrospinal fluid collection, as well as prior to euthanasia, animals were anesthetized with 80 mg/kg of ketamine and 10 mg/kg of xylazine administered via intraperitoneal and subcutaneous injections, respectively.

(ii) Postchallenge observations and body weight measurements.

Animals were observed every 6 h postchallenge until scheduled termination or until the animal was found dead or was euthanized because of its moribund condition. Signs of illness (i.e., dyspnea, forced abdominal respirations, unresponsiveness to touch or external stimuli) were monitored and recorded. Body weights were measured daily beginning on the day before the challenge (baseline) until the scheduled terminal endpoint or until the animal was found dead or euthanized because of moribundity. To determine if the mean weight at each postchallenge study day was significantly different from that at the baseline, a paired *t*-test analysis was performed.

(iii) Blood collection. Blood was collected by cardiac puncture or from the cranial vena cava. Blood from each animal was collected in serum separator tubes and sodium polyanethol sulfonate and EDTA tubes.

(iv) Bacterial burden assessment. For qualitative bacteremia assessment, 30 to 40 μ l of whole blood was inoculated onto blood agar plates and the plates were incubated at 37°C for a minimum of 48 h. A plate containing at least one colony with morphology consistent with *B. anthracis* was considered positive for *B. anthracis*. For quantitative assessment, 100 μ l of whole blood was plated in triplicate on tryptic soy agar (TSA). In addition, 10-fold serial dilutions were performed by transferring 100 μ l of whole blood or a previous dilution into 900 μ l of phosphate-buffered saline (PBS). A 100- μ l volume of each dilution prepared was plated in triplicate on TSA. Plates were incubated at 37°C for 16 to 24 h, bacterial colonies were enumerated, and the corresponding concentration (CFU/ml) was calculated.

For qualitative bacteremia assessment, estimates with 95% confidence intervals for the proportions of bacteremic animals were calculated within each group. For quantitative assessment, geometric means and 95% confidence intervals were calculated within each group. The limit of detection (LOD) for quantitative bacteremia was 100 CFU/ml. The concentrations reported to be below the LOD were recorded as 50 CFU/ml for the statistical analysis.

Quantitative PCR (qPCR) analysis for the presence of bacterial DNA was performed by the amplification of a small fragment within the coding region of the *rpoB* gene on the *B. anthracis* chromosome.

(v) Serum protective-antigen (PA) enzyme-linked immunosorbent

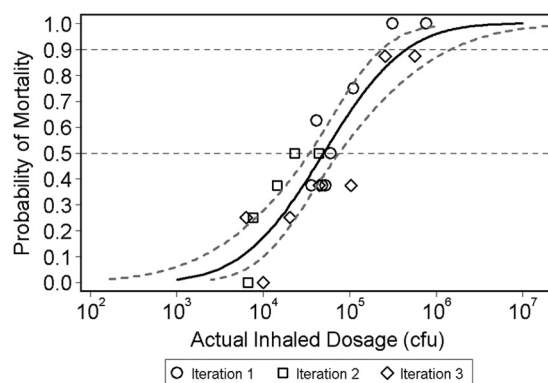


FIG 1 Dose-lethality curve obtained by using the log-transformed estimated inhaled dosage as the predictor variable. The LD₅₀ was determined in three iterations. Groups of animals were exposed to various doses with challenge dose levels in the second and third iterations based on the survival results from the previous iteration(s). In each iteration, guinea pigs were monitored for death twice daily for up to 21 days. The predicted curve from the probit model using data from all three iterations is plotted as a solid line, while the observed lethality are displayed as symbols by iteration. In addition, the upper and lower 95% confidence bounds on the predicted curve are shown as dashed lines. The two horizontal reference lines correspond to 50 and 90% mortality. The LD₅₀ for all three iterations combined was estimated at 5.01×10^4 spores per animal with a 95% confidence interval of 3.44×10^4 to 7.54×10^4 spores per animal.

TABLE 3 Estimated LD₅₀ and LD₉₀ for each iteration

Iteration(s)	Estimated no. of spores/animal (95% confidence interval)	
	LD ₅₀	LD ₉₀
I	5.27×10^4 (3.09×10^4 - 7.80×10^4)	1.79×10^5 (1.06×10^5 - 1.78×10^6)
II	3.13×10^4 (1.69×10^4 - 6.83×10^6)	2.01×10^5 (5.74×10^4 - 1.55×10^{14})
III	7.63×10^4 (3.69×10^4 - 1.94×10^5)	8.54×10^5 (2.92×10^5 - 1.36×10^7)
I, II, III	5.01×10^4 (3.44×10^4 - 7.54×10^4)	4.51×10^5 (2.35×10^5 - 1.47×10^6)

assay (ELISA). For detection of anthrax PA in the sera of infected animals, anti-PA IgG “capture antibody” (Battelle Memorial Institute, Columbus, OH) purified from recombinant PA (rPA)-vaccinated rabbit serum using a protein A column, followed by a PA column, was used to coat the wells of a 96-well plate at a concentration of 2 µg/ml. The plates were blocked at 37°C for 30 to 90 min with skim milk and then incubated at 37°C for 60 min with rabbit serum samples containing native PA (lot NR-164; Biode-

fense and Emerging Infections Research Resources Repository) or a reference standard and quality control samples consisting of rPA spiked differentially into naïve guinea pig serum. The PA was detected by incubating the plates at 37°C for 60 min with diluted goat PA antiserum, followed by incubation at 37°C for 60 min with a bovine anti-goat horseradish peroxidase-conjugated secondary antibody (Santa Cruz Biologicals, Santa Cruz, CA) and then a 2,2'-azinobis(3-ethylbenzothiazoline-6-

TABLE 4 Summary of mortality results

Animal ID	Group	Time to scheduled terminal endpoint	Time to death from median challenge time ^a	Outcome
136F	1	24 ± 1 h	27:24	Scheduled euthanasia
138F	1	24 ± 1 h	27:25	Scheduled euthanasia
172M	1	24 ± 1 h	27:36	Scheduled euthanasia
188M	1	24 ± 1 h	27:51	Scheduled euthanasia
144F	2	30 ± 1 h	30:02	Scheduled euthanasia
145F	2	30 ± 1 h	30:17	Scheduled euthanasia
178M	2	30 ± 1 h	30:29	Scheduled euthanasia
179M	2	30 ± 1 h	30:34	Scheduled euthanasia
141F	3	36 ± 1 h	36:00	Scheduled euthanasia
148F	3	36 ± 1 h	36:06	Scheduled euthanasia
175M	3	36 ± 1 h	36:18	Scheduled euthanasia
183M	3	36 ± 1 h	36:23	Scheduled euthanasia
140F	4	48 ± 1 h	47:45	Found dead
153F	4	48 ± 1 h	48:17	Scheduled euthanasia
181M	4	48 ± 1 h	48:21	Scheduled euthanasia
185M	4	48 ± 1 h	48:27	Scheduled euthanasia
139F	5	60 ± 1 h	59:44	Found dead
149F	5	60 ± 1 h	54:22	Moribund euthanasia
173M	5	60 ± 1 h	51:42	Found dead
182M	5	60 ± 1 h	59:44	Found dead
150F	6	72 ± 1 h	45:55	Found dead
151F	6	72 ± 1 h	66:10	Found dead
171M	6	72 ± 1 h	72:04	Scheduled euthanasia
176M	6	72 ± 1 h	54:01	Found dead
142F	7	96 ± 1 h	48:08	Moribund euthanasia
147F	7	96 ± 1 h	59:44	Found dead
184M	7	96 ± 1 h	51:42	Found dead
187M	7	96 ± 1 h	70:45	Found dead
131F	8	14 days	51:41	Found dead
132F	8	14 days	60:13	Moribund euthanasia
133F	8	14 days	59:44	Found dead
134F	8	14 days	59:59	Found dead
135F	8	14 days	54:01	Found dead
166M	8	14 days	48:01	Moribund euthanasia
167M	8	14 days	54:01	Found dead
168M	8	14 days	66:10	Found dead
169M	8	14 days	54:01	Found dead
143F	9	0 days	Not challenged	Scheduled euthanasia
146F	9	0 days	Not challenged	Scheduled euthanasia
174M	9	0 days	Not challenged	Scheduled euthanasia
186M	9	0 days	Not challenged	Scheduled euthanasia

^a Values are hours:minutes.

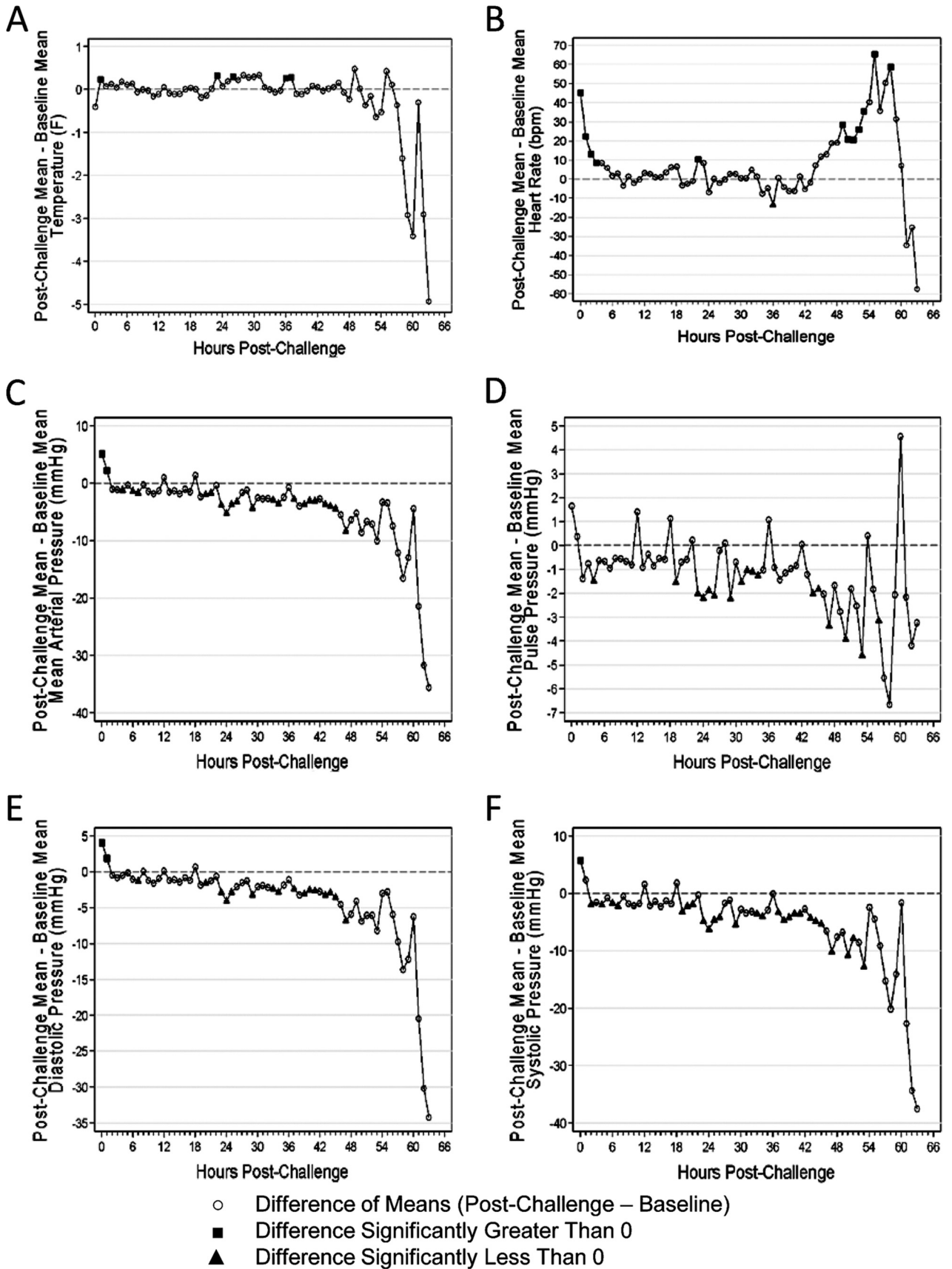


TABLE 5 Summary of the time to abnormal results for all telemetry parameters

Parameter	No. of abnormal animals/total	Proportion abnormal (exact 95% confidence interval)	Geometric mean time (h) to abnormality (95% confidence interval) ^a
Activity	0/9	0.00 (0.00–0.34)	— ^b
Temp	8/9	0.89 (0.52–1.00)	46.16 (34.75–57.56)
Heart rate	7/9	0.78 (0.40–0.97)	44.32 (26.78–61.86)
MAP	9/9	1.00 (0.66–1.00)	52.48 (48.01–56.95)
Pulse pressure	7/9	0.78 (0.40–0.97)	51.75 (45.15–58.35)
Diastolic BP	9/9	1.00 (0.66–1.00)	52.37 (49.44–55.29)
Systolic BP	9/9	1.00 (0.66–1.00)	53.92 (50.23–57.62)

^a These calculations include only animals that showed abnormal values.

^b —, No calculations were performed because the values of all of the animals were normal.

sulfonic acid) diammonium salt substrate and a stop solution (both from Kirkegaard and Perry Laboratories, Gaithersburg, MD).

The plates were read using a BioTek ELx800, SPECTRAMax PLUS³⁸⁴ at a wavelength of 405 nm with a reference wavelength of 490 nm, and the data were analyzed by using a four-parameter logistic-log (4PL) model to fit the eight-point calibration curve. The PA concentrations in unknown samples were determined by computer interpolation from the plot of the reference standard curve data (Softmax Pro; Molecular Devices). All PA ELISA observations reported to be below the LOD of 1.30 ng/ml were recorded as 0.65 ng/ml for the statistical analysis.

(vi) Hematology and clinical chemistry. Hematology assessment of whole-blood samples with an Advia 120 Hematology Analyzer (Siemens, Deerfield, IL) included the following parameters: red blood cell count (RBC), hemoglobin (HGB), hematocrit (HCT), mean corpuscular volume (MCV), mean corpuscular hemoglobin (MCH), mean corpuscular hemoglobin concentration (MCHC), red cell distribution width (RDW), platelet count (PLT), mean platelet volume (MPV), and total and differential white blood cell (WBC) count.

Serum samples were analyzed using an Advia 1200 Chemistry Analyzer (Siemens Medical Solutions Diagnostics, Tarrytown, NY) for serum proteins, liver function enzymes, kidney function parameters, electrolytes, and C-reactive protein (CRP).

Analysis-of-variance (ANOVA) models with an effect for group were fitted separately to each hematology and clinical chemistry parameter. These models were used to determine if the levels in each challenge group were significantly different from those in the control group. Hematology and clinical chemistry data from each challenged group were compared to those in the control group. An ANOVA model was fitted separately to each hematology parameter with an effect for group in order to check the model assumption of normality and to identify potential outliers. The models were fitted to log₁₀-transformed data.

(vii) Gross pathology and histopathology. Complete necropsies were performed on all guinea pigs found dead, euthanized because of their moribund condition, or euthanized at scheduled termination time points. Brains, hearts, large intestines (cecum, colon, and rectum), kidneys, livers, lungs, lymph nodes (bronchial, mediastinal, mandibular, and mesenteric), mammary glands, pancreases, small intestines (duodenum, jejunum, and ileum), spleens, and stomachs, as well as any other abnormal tissues and gross lesions, were collected. Tissue samples were preserved in 10% neutral buffered formalin, paraffin embedded, processed to slides, and stained with hematoxylin and eosin (HE). The microscopic findings were graded semiquantitatively. A numerical score (grades 1 through 4) was used to describe the average severity grade of each lesion, as well as the

extent of bacterial invasion of the tissue. Gross and microscopic diagnoses were entered into the PATH/TOX SYSTEM (Xybion Medical Systems Corporation, Cedar Knolls, NJ) for data tabulation and analysis.

(viii) Telemetry. One group of nine guinea pigs (four males and five females) was implanted with telemetry transmitters (TL10M2-C50-PT; Data Sciences International, St. Paul, MN) to collect data on the following parameters: body temperature, systolic blood pressure (BP), diastolic BP, mean arterial pressure (MAP), pulse pressure, heart rate, and activity. The data were recorded for a period 30 s every 15 min, beginning at 5 days prechallenge (baseline levels) and continuing until the animal was euthanized or succumbed to infection.

The mean value of each parameter measured by telemetry was computed every 15 min for 24 h (00:00, 00:15, . . . , 23:45) prechallenge (baseline). Data collected postchallenge were then baseline adjusted according to the associated clock time. One-hour averages were computed for the baseline-adjusted values such that, for example, the 1 a.m. average for a given study day included measurements recorded at 1:00, 1:15, 1:30, and 1:45. The standard deviation of all 1-h averages at the baseline was calculated for each animal and used to form the upper and lower limits for indications of abnormality. The upper limit was defined as 3 standard deviations above zero, while the lower limit was defined as 3 standard deviations below zero. A parameter was defined as abnormal if three consecutive baseline-adjusted 1-h averages were outside the upper or lower limit postchallenge. The time of onset of abnormality was defined as the time associated with the third abnormal value during the first occurrence of three consecutive abnormal values postchallenge.

Proportions of abnormal animals and exact 95% confidence intervals were calculated for each telemetry parameter. For those animals that became abnormal, the mean time to abnormality and 95% confidence intervals were also calculated for each telemetry parameter.

RESULTS

LD₅₀ determination. Using a nose-only aerosol exposure system, guinea pigs were challenged with inhaled doses of *B. anthracis* Ames spores ranging from 6.4×10^3 to 7.69×10^5 per animal (Table 2). Analysis of the mortality data showed that there was a statistically significant dose-response relationship ($P < 0.0001$), with higher dosages of the agent resulting in a higher probability of death (Fig. 1). The nose-only anthrax spore LD₅₀ for guinea pigs was found to be approximately 5.0×10^4 spores per animal (Table 3; Fig. 1). There was no impact on the LD₅₀ ($P = 0.11$) when

FIG 2 Changes in telemetric parameters postchallenge. Nine challenged animals were surgically implanted with telemetry transmitters and monitored for clinical signs of disease. The mean value for each parameter measured by telemetry was computed every 15 min for 24 h (00:00, 00:15, . . . , 23:45) prechallenge (baseline). The data collected postchallenge were then baseline adjusted according to the associated clock time. In these graphs, the mean differences that were significantly greater than zero are indicated by black squares, while the mean differences that were significantly less than zero are indicated by black triangles. The parameters monitored included temperature (A), heart rate (B), MAP (C), pulse pressure (D), diastolic BP (E), and systolic BP (F).

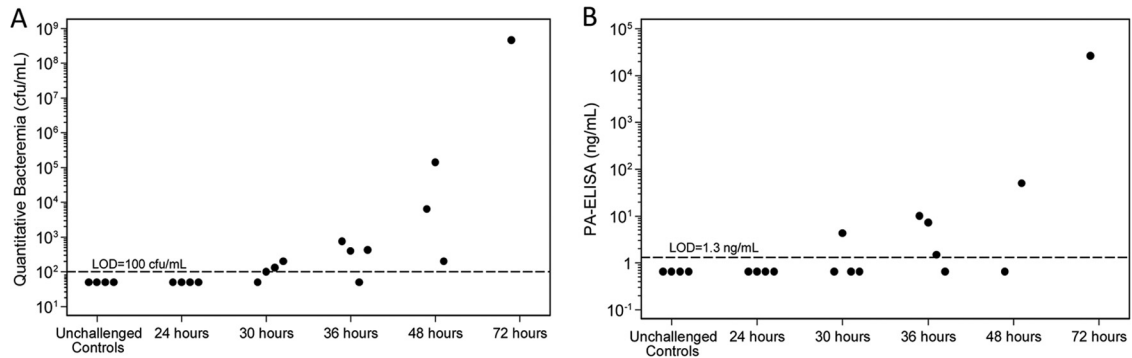


FIG 3 Bacterial and toxin levels postchallenge. (A) Quantitative bacteremia, A 100- μ l volume of whole blood was plated in triplicate on TSA. In addition, 10-fold serial dilutions were performed by transferring 100 μ l of whole blood or the previous dilution into 900 μ l of PBS. A 100- μ l volume of each dilution prepared was plated in triplicate on TSA. Plates were incubated at 37°C for 16 to 24 h, bacterial colonies were enumerated, and the corresponding concentration (CFU/ml) was calculated. (B) PA levels measured by ELISA. Plates were read, and the data were analyzed by using a 4PL model to fit the eight-point calibration curve. The PA concentrations in samples were determined by computer interpolation from the plot of the reference standard curve data.

animal gender was considered, nor was there an interaction between gender and inhaled dose ($P = 0.97$).

Natural history. (i) Aerosol challenge. The total inhaled dose was calculated from the impinger sample concentrations, sampling parameters, and exposure duration. The mean inhaled dose was 406 ± 13 LD₅₀ equivalents (based on the LD₅₀ determined in the experiment described above). The spray factor determined for

the spore lot used for these studies was different from the spray factors observed during the animal challenges (the spray factor was better during the animal challenges). This accounted for the observed difference between the actual challenge dose and the target dose. The mass median aerodynamic diameter was determined to be 1.21 μ m (with a geometric standard deviation of 1.28 μ m), indicating that the aerosol particle size was around the optimal size (~ 1 μ m) for delivery of the spores to alveoli (43).

(ii) Mortality, clinical signs, and body weights. Of the 37 anthrax-infected animals, 16 survived to scheduled termination time points, including all of the animals scheduled to be sacrificed at 24, 30, and 36 h postchallenge, 3 of 4 animals scheduled to be sacrificed at 48 h postchallenge, and 1 of 4 animals scheduled to be sacrificed at 72 h postchallenge (Table 4). The remaining 21 anthrax-infected animals were found dead or euthanized because of their moribund condition (Table 4). The time to death for these animals ranged between 46 and 71 h postchallenge, with a mean of 56 h.

Animals did not show any clinical signs of disease during the first 36 h postchallenge. Within a few hours after the appearance of symptoms, animals either died or reached a moribund condition and met the criteria for euthanasia. The clinical manifestations were consistent with inhalational anthrax and similar to those observed in the rabbit and NHP models, including labored breathing, cough, lacrimation, weakness, cyanosis, and lethargy. There was no significant change from the baseline weight in any animal postchallenge.

(iii) Telemetry data. Of nine animals implanted with telemetry transmitters, seven showed abnormal results for each of the telemetry parameters except activity (Fig. 2). The mean time to abnormal readings ranged from approximately 44 h postchallenge (increased heart rate) through approximately 54 h postchallenge (decreased systolic BP) (Table 5). In comparison to the baseline values, temperatures were significantly greater at 1, 23, 26, 36, and 37 h postchallenge. Heart rates were significantly elevated from the baseline during the first 3 h postchallenge and for 5 consecutive h beginning at 49 h postchallenge (Fig. 2). MAP, pulse pressure, diastolic BP, and systolic BP decreased significantly from the baseline levels between 20 and 51 h postchallenge and generally remained significantly lower than the baseline levels until death (Fig. 2). Activity was measured by adding up the number of move-

TABLE 6 Summary of hematologic changes in infected animals versus unchallenged controls

Parameter	Difference from unchallenged control (group 9) ^b				
	Group 1 (24 h)	Group 2 (30 h)	Group 3 (36 h)	Group 4 (48 h)	Group 6 (72 h)
RBC count ^a	–	–	–	–	++ ↓
Hemoglobin	–	–	–	–	+ ↓
Hematocrit ^a	–	–	–	–	+++ ↓
MCV	–	–	–	–	++ ↑
MCH	–	–	–	–	+++ ↑
MCHC	+ ↑	–	++ ↑	–	+++ ↑
RDW	–	–	–	–	+++ ↑
Platelet count	–	–	–	–	+++ ↑
MPV ^a	–	–	–	–	–
WBC ^a	–	–	–	+ ↑	+++ ↑
Heterophil count ^a	–	–	–	++ ↑	+++ ↑
Lymphocyte count	–	–	–	–	+++ ↑
N/L ratio ^a	–	–	–	++ ↑	+++ ↑
Monocyte count	–	–	–	–	+++ ↑
Eosinophil count ^a	–	–	–	–	–
Basophil count	–	–	–	–	+++ ↑

^a The values for this parameter were log transformed for the analysis.

^b Dunnett's two-sided P values were used for comparisons with the unchallenged control (group 9). Comparisons between group 6 and the unchallenged control (group 9) were based on one observation in group 6. Symbols: –, group mean (or geometric mean for log-transformed parameters) not significantly different ($P > 0.05$) from that of the unchallenged control (group 9); +, group mean (or geometric mean for log-transformed parameters) significantly different ($P < 0.05$) from that of the unchallenged control (group 9); ++, group mean (or geometric mean for log-transformed parameters) significantly different ($P < 0.01$) from that of the unchallenged control (group 9); +++, group mean (or geometric mean for log-transformed parameters) significantly different ($P < 0.001$) from that of the unchallenged control (group 9); ↑, group mean (or geometric mean for log-transformed parameters) significantly greater than that of the unchallenged control (group 9); ↓, group mean (or geometric mean for log-transformed parameters) significantly lower than that of the unchallenged control (group 9) at the 0.05 level.

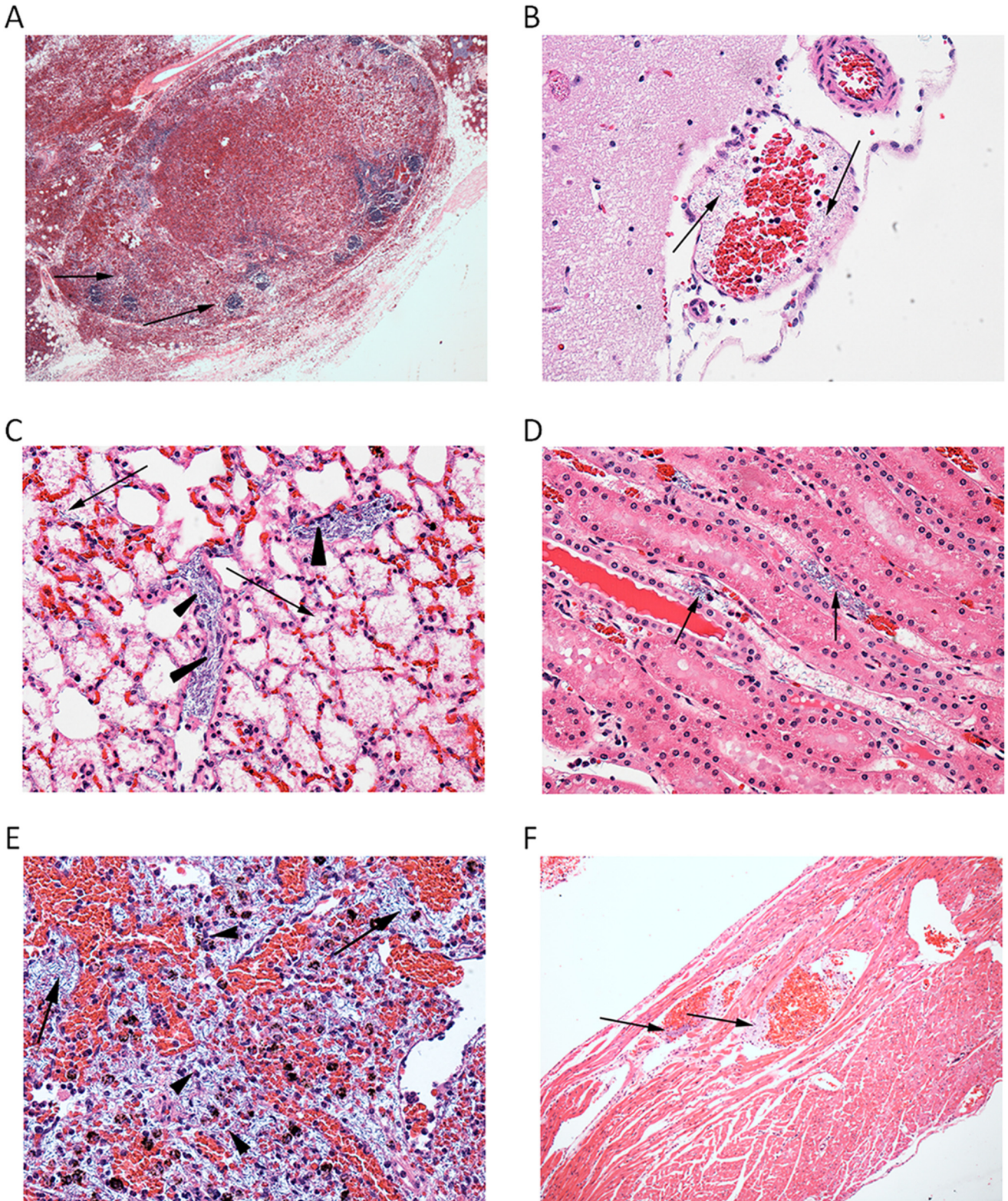


FIG 4 Histopathological findings. Tissue samples were preserved in 10% neutral buffered formalin, paraffin embedded, processed to slides, and stained with HE. Representative histopathological findings are shown. (A) Lymph node sinuses and extravascular tissues are filled with blood (hemorrhage), and only remnants of lymphoid follicles remain (arrows). HE staining, $\times 4$ magnification. (B) Brain, meninges. The blood vessel shown contains large, rod-shaped bacteria consistent with anthrax bacilli (arrows). HE staining, $\times 10$ magnification. (C) Alveoli filled with fibrin and edema (arrows) including pulmonary intravascular *B. anthracis* (arrowheads). HE staining, $\times 40$ magnification. (D) Renal vessels containing anthrax bacilli (arrows). HE staining, $\times 40$ magnification. (E) Spleen tissue showing sinusoidal anthrax bacilli and degenerate and viable heterophils (arrows). HE staining, $\times 40$ magnification. (F) Heart tissue showing anthrax bacilli within coronary vessels (arrows). HE staining, $\times 10$ magnification.

TABLE 7 Aerosol anthrax spore LD₅₀s for laboratory animals and humans

Species	Route	Strain(s)	LD ₅₀	Reference(s)
Guinea pig	Intramuscular injection	Ames	1.0×10^2	65
Guinea pig	Intranasal instillation	Ames	6.0×10^5	47
Guinea pig	Whole-body aerosol exposure	NH-6, Vollum 1B	6.5×10^2 – 7.0×10^4	48
Guinea pig	Nose-only aerosol exposure	Ames	5.0×10^4	This study
Rabbit	Muzzle	Ames	1.1×10^5	8
Common marmoset	Head-only aerosol exposure	Ames	1.5×10^3	24
Cynomolgus macaque	Head-only aerosol exposure	Ames	6.2×10^4	15
Rhesus macaque	Head-only aerosol exposure	Ames	5.5×10^4	13
Human (estimates)	Aerosol	— ^a	2.0×10^3 – 5.5×10^4	49–52

^a —, Modeling is based in part on the isolate from the 1979 accidental spore release in Sverdlovsk, USSR.

ments over the telemetry sampling period as detected by the telemetry receiver.

(iv) **Bacterial burden and toxemia.** Inhalational anthrax in mammalian species is characterized by the dissemination of bacilli via the circulatory system, resulting in septicemia and toxemia that lead to secondary invasion of internal organs and tissues, including the central nervous system, culminating in a fatal outcome (44). Accordingly, the bacterial burden in blood was assessed in this study. The first positive blood cultures were detected as early as 24 h postchallenge (one of four animals was positive in the qualitative bacteremia assessment), and the proportion of bacteremic animals, as well as bacterial counts, increased as the disease progressed (Fig. 3A). The results of the qPCR analysis were consistent with the quantitative bacteremia data (data not shown).

PA is one of the key virulence factors in a *B. anthracis* infection, as it combines with edema factor to form edema toxin (ET) and with lethal factor to form lethal toxin (LT). Thus, measurement of PA is considered an appropriate marker of anthrax and has been used as a biomarker of disease in the NHP and rabbit models (34). In this study, PA was first detected in the serum at 30 h postchallenge and its levels continued to increase with time (Fig. 3B).

(v) **Hematology and clinical chemistry.** Hematologic parameters can potentially serve as important markers of local and systemic inflammation induced by an infection, vascular barrier disruption (5), and immune suppression (66) caused by the *B. anthracis* LT. However, humans rarely exhibit drastic hematological changes during early stages of anthrax (67). Similarly, during the first 48 h postchallenge, only minor fluctuations in the red blood cell parameters, judged to be not biologically relevant, were observed in guinea pigs (Table 6). One animal that survived until scheduled termination at 72 h postchallenge, as well as four animals from which blood was collected prior to euthanasia because of their moribund condition, showed significant decreases in RBC, HGB, and HCT levels; increases in MCH, MCHC, and RDW levels; and elevated PLT counts. Heterophil leukocytosis, lymphocytosis or lymphopenia, and increased heterophil/lymphocyte ratios, as well as occasional monocytosis, eosinophilia, and basophilia, were also noted in these five animals.

No clinically significant changes in clinical chemistry parameters were observed (data not shown).

(vi) **Pathology.** Necropsy examination revealed no gross lesions in animals that died or were euthanized prior to 48 h postchallenge. In contrast, animals that died or were euthanized at later time points exhibited changes consistent with anthrax, including enlarged and darkened bronchial, mediastinal, and/or

mesenteric lymph nodes. These lesions corresponded microscopically to mild-to-moderate hemorrhage.

Microscopic findings in animals sacrificed at 24 h postchallenge included minimal hemorrhage and interstitial nonsuppurative inflammation in the lungs; minimal-to-mild mandibular, mediastinal, and mesenteric lymph node and splenic lymphocyte depletion/lymphocytolysis; and/or hemorrhage and hepatocellular necrosis. A minimal presence of bacteria in the liver was observed in this group of animals. The nonsuppurative inflammation was likely preexisting. Animals sacrificed at 30 h postchallenge exhibited minimal nonsuppurative inflammation in the lungs and minimal lymphocyte depletion/lymphocytolysis in the regional and mesenteric lymph nodes and spleen. Minimal-to-mild hemorrhage was observed in the mediastinal (Fig. 4A) and mandibular lymph nodes. Submucosal edema was present in the stomach of one animal. In livers, hepatocellular necrosis with minimal bacteria was also noted. By 36 h postchallenge, bacteria (minimal and primarily intravascular) were observed in the meninges of the brain. Figure 4B shows meningeal blood vessels that contain bacilli. Minimal-to-mild lymphoid destruction (lymphocyte depletion/lymphocytolysis) occurred in the mediastinal and mesenteric lymph nodes and in the spleen. No other organs, including the lungs, were affected in animals sacrificed at this time point. Similar findings but with increased lesion severity were noted in animals sacrificed at later time points.

The microscopic lesions found in the 21 guinea pigs that did not survive to their scheduled termination time points were typical of disseminated anthrax and included the presence of bacilli, suppurative heterophilic inflammation, edema, fibrin, necrosis, and/or hemorrhage in the spleen, lungs, and lymph nodes (bronchial, mediastinal, mandibular, and mesenteric). The lungs exhibited alveolar edema and hemorrhage with interstitial inflammation (Fig. 4C). Bacteria were present in pulmonary interstitial blood vessels, alveoli (rarely), and hepatic sinusoids. Minimal hepatocellular necrosis was present in the liver of one animal. Lymphocyte depletion and/or lymphocytolysis were present in most lymph nodes and prevailed in the bronchial and mediastinal lymph nodes and the spleen. Lymphocytolysis was characterized by increased apoptotic lymphocytes within and outside germinal centers. Bacilli were abundant in renal vessels (Fig. 4D) and the splenic red pulp and lymph node sinuses (Fig. 4E). Bacilli were also present in the vasculature of the pancreas, mammary glands, heart (Fig. 4F), and gastrointestinal tissues and occasionally in meningeal vessels.

DISCUSSION

Animal models of diseases that afflict humans are critical tools for the development of medical countermeasures against life-threatening conditions, such as inhalational anthrax, for which clinical evaluation of efficacy is not feasible. The use of an animal model for assessment of the efficacy of a medical countermeasure is contingent upon a thorough characterization of the course and manifestation of the disease of interest in that animal model. This is particularly important in cases where an established and universally accepted model is not suitable for the evaluation of a particular drug or vaccine and an alternative model needs to be developed. In such cases, assessment of the natural history of the disease under appropriate and controlled conditions similar to those used for the established models is essential.

In the case of experimental inhalational anthrax, the standard conditions used in anthrax challenge studies with rabbits and NHPs aimed at the evaluation of anthrax vaccines and therapeutics include the use of the highly virulent Ames strain of *B. anthracis*, which is known to be highly virulent in humans (36); standardized and validated spore preparation and characterization methods that ensure consistency of the challenge material (39, 45, 46); an appropriate target challenge dose (200 LD₅₀) that ensures universal lethality in untreated animals; and an appropriate aerosol exposure system that ensures the delivery of aerosolized spores to the lung while minimizing nonpulmonary exposure. Therefore, this study was focused on the natural history of inhalational anthrax in guinea pigs under these standardized conditions, as well as on comparing the clinical signs, disease progression, and pathology observed in guinea pigs with those previously described for human disease and other animal models.

As summarized in Table 7, the inhaled LD₅₀ of the Ames strain of *B. anthracis* in guinea pigs in a nose-only exposure system was determined to be somewhat different from the previously reported LD₅₀s obtained with the whole-body exposure system (48) and intranasal instillation (47). However, it is comparable to the estimated human LD₅₀ (49–51, 53), as well as to the published muzzle-only LD₅₀ for New Zealand White rabbits (8) and the head-only LD₅₀ for rhesus and cynomolgus macaques (13–15, 35), which indicates that guinea pig sensitivity to *B. anthracis* infection following inhalation exposure is similar to that in the established animal models.

It is believed that cardiovascular dysfunction, including decreased cardiac output, hypotension, and an altered heart rate, caused by the synergistic effect of LT and ET results in toxic (hypovolemic) shock in humans (54, 55). Telemetry data clearly demonstrate a decline of cardiovascular functions in guinea pigs reflecting the development of septic shock and death within several hours, which is not uncommon in humans (3) and correlates with previous findings in rabbits (9, 56) and African green monkeys (57).

Depending on the exposure dose and the severity and duration of the disease, there is wide variation in lesions associated with inhalational anthrax in humans (58). Postmortem findings reported in human cases include peripheral transudate-surrounded fibrin-rich edema, necrosis of arteries and veins leading to hemorrhages, displacement of infiltrating tissue resulting in necrosis of mediastinal lymph nodes, mediastinitis, pneumonia, pleural effusions, mesenteric lymphadenitis, multiple gastrointestinal submucosal lesions, and apoptosis of lymphocytes (58–60).

Various rodent and nonrodent species have been used as animal models of inhalational anthrax. The mouse model has been used to study the pathogenesis of *B. anthracis* infection and host-pathogen interactions, as well as to generate proof-of-concept data with anthrax countermeasures. However, the mouse is not very predictive of pulmonary anthrax in humans (61). This is due primarily to the fact that immunocompetent mice are resistant to infection with nonencapsulated toxinogenic strains such as the Sterne strain (62). Complement-deficient mouse models, such as A/J and DBA/2, are susceptible to the effects of LT (63); however, they do not exhibit the typical pathological changes observed in humans, guinea pigs, rabbits, and NHPs (7, 18). Although a rat *in vivo* LT neutralization model has been developed and used to evaluate antitoxin therapeutics (64), rats are highly resistant to *B. anthracis* spore exposure (estimated LD₅₀ of 1×10^6) and are therefore not considered an appropriate model for the study of inhalational anthrax (17).

In contrast, guinea pigs, rabbits, and several species of NHPs have been shown to be predictive of inhalational anthrax in humans (18). Both rabbits and guinea pigs rapidly develop fulminant systemic disease, with death occurring within 2 to 4 days postchallenge (8, 18), as shown with guinea pigs in this study. Histopathological findings in these models include necrotizing lymphadenitis, splenitis, pneumonia, vasculitis, hemorrhage, congestion, and edema in multiple tissues (18). In NHPs, pathology findings typically include congestion, edema, fibrin, hemorrhage, necrosis, infiltrates of acute inflammatory cells, and vasculitis in the lungs, lymph nodes, spleen, and meninges. In addition, the brain, adrenal glands, mesentery, liver, gastrointestinal tract, mediastinum, and urogenital organs are commonly affected in NHPs (14, 15, 18, 24).

This study showed close similarities between the natural history of experimental inhalational anthrax disease in guinea pigs exposed to aerosolized *B. anthracis* spores under standard conditions (200 LD₅₀, Ames strain, nose-only exposure, etc.) and that of the established rabbit and NHP models. By demonstrating the similarity of the pathophysiology and pathology of pulmonary anthrax disease in guinea pigs to those of the disease in humans, this study supports the use of this model as an alternative small-animal model for assessment of the efficacy of anthrax countermeasures.

ACKNOWLEDGMENTS

We thank Louise M. Pitt for valuable scientific advice and critical review of the manuscript. We are grateful to Sarah E. Szarowicz and Tyler D. Laudenslager for editorial review. We also thank Neil Gibson, Jared Wilcox, Amanda Jellick, Kassandra Bach, Phyllis Herr-Calomeni, and Pauline Vales for their technical contribution during the execution of this study.

This project was funded in whole or in part with federal funds from the Biomedical Advanced Research and Development Authority, Department of Health and Human Services, in conjunction with the National Institute of Allergy and Infectious Diseases, National Institutes of Health, Department of Health and Human Services, under contract HHSN272200800051C.

REFERENCES

1. Brachman PS. 1980. Inhalation anthrax. *Ann. N. Y. Acad. Sci.* 353:83–93.
2. Penn CC, Klotz SA. 1997. Anthrax pneumonia. *Semin. Respir. Infect.* 12:28–30.
3. Shafazand S, Doyle R, Ruoss S, Weinacker A, Raffin TA. 1999. Inhalational anthrax: epidemiology, diagnosis, and management. *Chest* 116: 1369–1376.

4. Holty JE, Bravata DM, Liu H, Olshen RA, McDonald KM, Owens DK. 2006. Systematic review: a century of inhalational anthrax cases from 1900 to 2005. *Ann. Intern. Med.* 144:270–280.
5. Golden HB, Watson LE, Lal H, Verma SK, Foster DM, Kuo SR, Sharma A, Frankel A, Dostal DE. 2009. Anthrax toxin: pathologic effects on the cardiovascular system. *Front. Biosci.* 14:2335–2357.
6. Phipps AJ, Premanandan C, Barnewall RE, Lairmore MD. 2004. Rabbit and nonhuman primate models of toxin-targeting human anthrax vaccines. *Microbiol. Mol. Biol. Rev.* 68:617–629.
7. Goossens PL. 2009. Animal models of human anthrax: the quest for the holy grail. *Mol. Aspects Med.* 30:467–480.
8. Zaucha GM, Pitt LM, Estep J, Ivins BE, Friedlander AM. 1998. The pathology of experimental anthrax in rabbits exposed by inhalation and subcutaneous inoculation. *Arch. Pathol. Lab. Med.* 122:982–992.
9. Lawrence WS, Hardcastle JM, Brining DL, Weaver LE, Ponce C, Whorton EB, Peterson JW. 2009. The physiologic responses of Dutch belted rabbits infected with inhalational anthrax. *Comp. Med.* 59:257–265.
10. Berdjis CC, Gleiser CA, Hartmen HA, Kuehne RW, Gochenour WS. 1962. Pathogenesis of respiratory anthrax in *Macaca mulatta*. *Br. J. Exp. Pathol.* 43:515–524.
11. Gleiser CA, Berdjis CC, Hartman HA, Gochenour WS. 1963. Pathology of experimental respiratory anthrax in *Macaca mulatta*. *Br. J. Exp. Pathol.* 44:416–426.
12. Henderson DW, Peacock S, Belton FC. 1956. Observations on the prophylaxis of experimental pulmonary anthrax in the monkey. *J. Hyg. (Lond.)* 54:28–36.
13. Ivins BE, Pitt ML, Fellows PF, Farchaus JW, Benner GE, Waag DM, Little SF, Anderson GW, Jr, Gibbs PH, Friedlander AM. 1998. Comparative efficacy of experimental anthrax vaccine candidates against inhalation anthrax in rhesus macaques. *Vaccine* 16:1141–1148.
14. Fritz DL, Jaax NK, Lawrence WB, Davis KJ, Pitt ML, Ezzell JW, Friedlander AM. 1995. Pathology of experimental inhalation anthrax in the rhesus monkey. *Lab. Invest.* 73:691–702.
15. Vasconcelos D, Barnewall R, Babin M, Hunt R, Estep J, Nielsen C, Carnes R, Carney J. 2003. Pathology of inhalation anthrax in cynomolgus monkeys (*Macaca fascicularis*). *Lab. Invest.* 83:1201–1209.
16. Twenhafel NA, Leffel E, Pitt ML. 2007. Pathology of inhalational anthrax infection in the African green monkey. *Vet. Pathol.* 44:716–721.
17. Leffel EK, Pitt LM. 2006. Anthrax, p 77–94. *In* Swearingen JR (ed), *Biodefense: research methodology and animal models*. CRC Press, Boca Raton, FL.
18. Twenhafel NA. 2010. Pathology of inhalational anthrax animal models. *Vet. Pathol.* 47:819–830.
19. Rankin R, Pontarollo R, Ioannou X, Krieg AM, Hecker R, Babiuk LA, van Drunen Littel-van den Hurk S. 2001. CpG motif identification for veterinary and laboratory species demonstrates that sequence recognition is highly conserved. *Antisense Nucleic Acid Drug Dev.* 11:333–340.
20. Ross JM. 1957. The pathogenesis of anthrax following the administration of spores by the respiratory route. *J. Pathol. Bacteriol.* 73:485–494.
21. Ivins BE, Ezzell JW, Jr, Jemski J, Hedlund KW, Ristorph JD, Leppa SH. 1986. Immunization studies with attenuated strains of *Bacillus anthracis*. *Infect. Immun.* 52:454–458.
22. Turnbull PC, Broster MG, Carman JA, Manchee RJ, Melling J. 1986. Development of antibodies to protective antigen and lethal factor components of anthrax toxin in humans and guinea pigs and their relevance to protective immunity. *Infect. Immun.* 52:356–363.
23. Little SF, Knudson GB. 1986. Comparative efficacy of *Bacillus anthracis* live spore vaccine and protective antigen vaccine against anthrax in the guinea pig. *Infect. Immun.* 52:509–512.
24. Lever MS, Stagg AJ, Nelson M, Pearce P, Stevens DJ, Scott EA, Simpson AJ, Fulop MJ. 2008. Experimental respiratory anthrax infection in the common marmoset (*Callithrix jacchus*). *Int. J. Exp. Pathol.* 89:171–179.
25. Brachman PS, Kaufman AF, Dalldorf FG. 1966. Industrial inhalation anthrax. *Bacteriol. Rev.* 30:646–659.
26. Dalldorf FG, Kaufmann AF, Brachman PS. 1971. Woolsorters' disease. An experimental model. *Arch. Pathol.* 92:418–426.
27. Daya M, Nakamura Y. 2005. Pulmonary disease from biological agents: anthrax, plague, Q. fever, and tularemia. *Crit. Care Clin.* 21:747–763, vii.
28. Guarner J, Zaki SR. 2006. Histopathology and immunohistochemistry in the diagnosis of bioterrorism agents. *J. Histochem. Cytochem.* 54:3–11.
29. Misra RP. 1991. Manual for the production of anthrax and blackleg vaccines. FAO animal production and health paper 87. Food and Agriculture Organization of the United Nations, Rome, Italy. <http://www.fao.org/docrep/004/T0278E/T0278E00.htm>.
30. Ivins B, Fellows P, Pitt L, Estep J, Farchaus J, Friedlander A, Gibbs P. 1995. Experimental anthrax vaccines: efficacy of adjuvants combined with protective antigen against an aerosol *Bacillus anthracis* spore challenge in guinea pigs. *Vaccine* 13:1779–1784.
31. Altbourn Z, Gozes Y, Barnea A, Pass A, White M, Kobiler D. 2002. Postexposure prophylaxis against anthrax: evaluation of various treatment regimens in intranasally infected guinea pigs. *Infect. Immun.* 70:6231–6241.
32. Stephenson EH, Moeller RB, York CG, Young HW. 1988. Nose-only versus whole-body aerosol exposure for induction of upper respiratory infections of laboratory mice. *Am. Ind. Hyg. Assoc. J.* 49:128–135.
33. Phalen RF, Mannix RC, Drew RT. 1984. Inhalation exposure methodology. *Environ. Health Perspect.* 56:23–34.
34. Migone TS, Subramanian GM, Zhong J, Healey LM, Corey A, Devalaraja M, Lo L, Ullrich S, Zimmerman J, Chen A, Lewis M, Meister G, Gillum K, Sanford D, Mott J, Bolmer SD. 2009. Raxibacumab for the treatment of inhalational anthrax. *N. Engl. J. Med.* 361:135–144.
35. Friedlander AM, Welkos SL, Pitt ML, Ezzell JW, Worsham PL, Rose KJ, Ivins BE, Lowe JR, Howe GB, Mikesell P, et al. 1993. Postexposure prophylaxis against experimental inhalation anthrax. *J. Infect. Dis.* 167:1239–1243.
36. Ravel J, Jiang L, Stanley ST, Wilson MR, Decker RS, Read TD, Worsham P, Keim PS, Salzberg SL, Fraser-Liggett CM, Rasko DA. 2009. The complete genome sequence of *Bacillus anthracis* Ames "Ancestor". *J. Bacteriol.* 191:445–446.
37. Inglesby TV, Henderson DA, Bartlett JG, Ascher MS, Eitzen E, Friedlander AM, Hauer J, McDade J, Osterholm MT, O'Toole T, Parker G, Perl TM, Russell PK, Tonat K. 1999. Anthrax as a biological weapon: medical and public health management. Working Group on Civilian Biodefense. *JAMA* 281:1735–1745.
38. Inglesby TV, O'Toole T, Henderson DA, Bartlett JG, Ascher MS, Eitzen E, Friedlander AM, Gerberding J, Hauer J, Hughes J, McDade J, Osterholm MT, Parker G, Perl TM, Russell PK, Tonat K. 2002. Anthrax as a biological weapon, 2002: updated recommendations for management. *JAMA* 287:2236–2252.
39. Kao LM, Bush K, Barnewall R, Estep J, Thalacker FW, Olson PH, Drusano GL, Minton N, Chien S, Hemeryck A, Kelley MF. 2006. Pharmacokinetic considerations and efficacy of levofloxacin in an inhalational anthrax (postexposure) rhesus monkey model. *Antimicrob. Agents Chemother.* 50:3535–3542.
40. Guyton AC. 1947. Measurement of the respiratory volumes of laboratory animals. *Am. J. Physiol.* 150:70–77.
41. Fieller EC. 1944. A fundamental formula in the statistics of biological assay, and some applications. *Q. J. Pharm. Pharmacol.* 17:117–123.
42. Finney DJ. 1971. *Probit analysis*, 3rd ed. Cambridge University Press, New York, NY.
43. Schlesinger RB. 1985. Comparative deposition of inhaled aerosols in experimental animals and humans: a review. *J. Toxicol. Environ. Health* 15:197–214.
44. Dixon TC, Meselson M, Guillemin J, Hanna PC. 1999. Anthrax. *N. Engl. J. Med.* 341:815–826.
45. Austin JL, Barnewall RE, Sanford DC, Stark GV. 2009. Impact of *Bacillus anthracis* spore preparation on aerosol performance. *Proceedings of Aerobiology in Biodefense III*, Cumberland, MD.
46. Austin JL, Guistino DJ, Stark GV, Barnewall RE, Syar ES, Hunt RE. 2009. The impact of storage duration on critical *Bacillus anthracis* Ames spores characteristics. *Proceedings of the 7th ASM Biodefense and Emerging Diseases Research Meeting*, Baltimore, MD.
47. Peterson JW, Comer JE, Noffsinger DM, Wenglikowski A, Walberg KG, Chatuev BM, Chopra AK, Stanberry LR, Kang AS, Scholz WW, Sircar J. 2006. Human monoclonal anti-protective antigen antibody completely protects rabbits and is synergistic with ciprofloxacin in protecting mice and guinea pigs against inhalation anthrax. *Infect. Immun.* 74:1016–1024.
48. Day WC, Bailey RR, TePaske GH, Wallace HC. 1962. Immunological studies with *Bacillus anthracis*. I. *Bacillus anthracis* aerosol challenge of guinea pigs vaccinated with protective antigen. U.S. Army Biological Laboratories, Fort Detrick, MD. Technical Memorandum 24. <http://www.dtic.mil/dtic/tr/fulltext/u2/285614.pdf>.
49. Cieslak TJ, Eitzen EM, Jr. 1999. Clinical and epidemiologic principles of anthrax. *Emerg. Infect. Dis.* 5:552–555.

50. Wilkening DA. 2006. Sverdlovsk revisited: modeling human inhalation anthrax. *Proc. Natl. Acad. Sci. U. S. A.* **103**:7589–7594.
51. Wilkening DA. 2008. Modeling the incubation period of inhalational anthrax. *Med. Decis. Making.* **28**:593–605.
52. Franz DR, Jahrling PB, Friedlander AM, McClain DJ, Hoover DL, Byrne WR, Pavlin JA, Christopher GW, Eitzen EM, Jr. 1997. Clinical recognition and management of patients exposed to biological warfare agents. *JAMA* **278**:399–411.
53. Franz DR, Jahrling PB, McClain DJ, Hoover DL, Byrne WR, Pavlin JA, Christopher GW, Cieslak TJ, Friedlander AM, Eitzen EM, Jr. 2001. Clinical recognition and management of patients exposed to biological warfare agents. *Clin. Lab. Med.* **21**:435–473.
54. Li Y, Sherer K, Cui X, Eichacker PQ. 2007. New insights into the pathogenesis and treatment of anthrax toxin-induced shock. *Expert Opin. Biol. Ther.* **7**:843–854.
55. Watson LE, Mock J, Lal H, Lu G, Bourdeau RW, Tang WJ, Leppla SH, Dostal DE, Frankel AE. 2007. Lethal and edema toxins of anthrax induce distinct hemodynamic dysfunction. *Front. Biosci.* **12**:4670–4675.
56. Lawrence WS, Marshall JR, Zavala DL, Weaver LE, Baze WB, Moen ST, Whorton EB, Gourley RL, Peterson JW. 2011. Hemodynamic effects of anthrax toxins in the rabbit model and the cardiac pathology induced by lethal toxin. *Toxins* **3**:721–736.
57. Rossi CA, Ulrich M, Norris S, Reed DS, Pitt LM, Leffel EK. 2008. Identification of a surrogate marker for infection in the African green monkey model of inhalation anthrax. *Infect. Immun.* **76**:5790–5801.
58. Grinberg LM, Abramova FA, Yampolskaya OV, Walker DH, Smith JH. 2001. Quantitative pathology of inhalational anthrax I: quantitative microscopic findings. *Mod. Pathol.* **14**:482–495.
59. Abramova FA, Grinberg LM, Yampolskaya OV, Walker DH. 1993. Pathology of inhalational anthrax in 42 cases from the Sverdlovsk outbreak of 1979. *Proc. Natl. Acad. Sci. U. S. A.* **90**:2291–2294.
60. Guarner J, Jernigan JA, Shieh WJ, Tatti K, Flannagan LM, Stephens DS, Popovic T, Ashford DA, Perkins BA, Zaki SR. 2003. Pathology and pathogenesis of bioterrorism-related inhalational anthrax. *Am. J. Pathol.* **163**:701–709.
61. Lipscomb MF, Hutt J, Lovchik J, Wu T, Lyons CR. 2010. The pathogenesis of acute pulmonary viral and bacterial infections: investigations in animal models. *Annu. Rev. Pathol.* **5**:223–252.
62. Welkos SL, Keener TJ, Gibbs PH. 1986. Differences in susceptibility of inbred mice to *Bacillus anthracis*. *Infect. Immun.* **51**:795–800.
63. Loving CL, Kennett M, Lee GM, Grippe VK, Merkel TJ. 2007. Murine aerosol challenge model of anthrax. *Infect. Immun.* **75**:2689–2698.
64. Ezzell JW, Ivins BE, Leppla SH. 1984. Immunoelectrophoretic analysis, toxicity, and kinetics of in vitro production of the protective antigen and lethal factor components of *Bacillus anthracis* toxin. *Infect. Immun.* **45**:761–767.
65. Fellows PF, Linscott MK, Ivins BE, Pitt ML, Rossi CA, Gibbs PH, Friedlander AM. 2001. Efficacy of a human anthrax vaccine in guinea pigs, rabbits, and rhesus macaques against challenge by *Bacillus anthracis* isolates of diverse geographical origin. *Vaccine* **19**:3241–3247.
66. Baldari CT, Tonello F, Paccani SR, Montecucco C. 2006. Anthrax toxins: a paradigm of bacterial immune suppression. *Trends Immunol.* **27**:434–440.
67. Jernigan JA, Stephens DS, Ashford DA, Omenaca C, Topiel MS, Galbraith M, Tapper M, Fisk TL, Zaki S, Popovic T, Meyer RF, Quinn CP, Harper SA, Fridkin SK, Sejvar JJ, Shepard CW, McConnell M, Guarner J, Shieh WJ, Malecki JM, Gerberding JL, Hughes JM, Perkins BA. 2001. Bioterrorism-related inhalational anthrax: the first 10 cases reported in the United States. *Emerg. Infect. Dis.* **7**:933–944.